Sound Speed Variability over Bay of Bengal from Argo Observations (2011-2020)

1st Sudip Jana
Department of Mathematics
Adamas University
Kolkata, India
sudip.ocn@gmail.com

2nd Avijit Gangopadhyay
School for Marine Science and Technology
University of Massachusetts Dartmouth
Dartmouth, MA, USA
avijit.gangopadhyay@umassd.edu

3rd Patrick J. Haley, Jr.
Department of Mechanical Engineering
Massachusetts Institute of Technology
Cambridge, MA, USA
phaley@mit.edu

4th Pierre F. J. Lermusiaux
Department of Mechanical Engineering
Massachusetts Institute of Technology
Cambridge, MA, USA
pierrel@mit.edu

OCEANS 2022 - Chennai | 978-1-6654-1821-8/22/$31.00 ©2022 IEEE | DOI: 10.1109/OCEANSChennai45887.2022.9775509

***Abstract*—In this paper, we study the spatio-temporal variability of the sound speed in the Bay of Bengal (BoB) estimated from the Argo observation data during 2011 - 2020. We perform domain-wide and region specific analysis of the sound speed structure and identify the regions and times of higher variabilities. The domain-wide spatio-temporal variability in the sound speed is maximum in the thermocline layers near 110 m depth. This variability is smaller at around 35-40m depth but increases in the surface layers. The regions of higher temporal and spatial variability vary with depth and time. In the surface layers, the variability is large in the northern part of the Bay but in the subsurface and the layers underneath, it is large along the entire western boundary from the north to south. Due to the combined impact of temperature inversion and the positive salinity gradient, the northern BoB experiences a significant positive vertical gradient in sound speed above the sonic layer depth (SLD) during the postmonsoon and winter periods. This gradient supports strong surface ducting and formation of the shadow zone below the SLD.**

Keywords—Sound speed variability, Bay of Bengal, Argo data, Sonic layer depth, Surface duct, Uncertainty characterization

I. INTRODUCTION

Underwater sound propagation has many important implications in acoustic communication, detecting underwater objects, and observing and monitoring the ocean interior and different oceanic processes. The analysis of the sound speed structure and its variability is essential to understand and predict the underwater refraction of sound and hence the formation of surface sound duct and shadow zone. The sound speed in the ocean depends on temperature, salinity and pressure and increases with all these three parameters. Among these three parameters, the temperature and salinity vary widely over space and time depending upon different oceanic and atmospheric conditions. In general the temperature plays the dominant role in controlling the variability in sound speed. However, the salinity impact becomes important in the regions where the salinity contrast is very large. The Bay of Bengal (BoB) is one such region that realizes a remarkable spatial and seasonal contrast in both temperature and salinity due to multiple factors.

The excess freshwater influx, intrusion of equatorial currents, seasonally reversing western boundary currents, eddies, basin to sub-basic scale gyres, and equatorial remote forcing substantially modulate the thermohaline structure and its variability in the BoB. The enormous amount of freshwater input from the monsoon rain and the runoff of a number of rivers results in extreme surface freshening in the northern BoB [1]–[6], which leads to the formation of barrier layer and temperature inversions [7]–[11]. The northward flowing Western Boundary Current (WBC) during spring carries salty water towards the north [12] – [14] while the southward flowing East India Coastal Current (EICC) carries low-saline water from the north to the south [4], [15]. The boundary currents and associated eddies lead to significant variability in the thermocline region. The southwest monsoon wind results in upwelling of colder subsurface water to the surface along the west coast during the summer [16]. The BoB remains populated by several eddies of shorter to longer time scales throughout the year. The intrusion of Southwest Monsoon Current (SMC) through the southwest corner during the monsoon period supplies warm and salty water that helps maintain the salinity balance in the BoB [17], [18]. The equatorial remote forcing, such as, the upwelling and downwelling Kelvin waves modulates the currents and the thermohaline structure [19]. All these factors affect the thermohaline structure of different parts of the BoB and eventually affect the sound speed of this region. Understanding of the spatial and seasonal distribution of the sound speed variability is useful for ocean acoustic modeling, sensing, and data assimilation [20]–[23]. Therefore, it is worthwhile to study the sound speed variability in the BoB.

A number of previous studies investigates different aspects of the BoB and Arabian Sea sound speed structures. Reference [24] studied the sound speed structure in the BoB and the Arabian Sea using the Levitus annual climatology. Reference [25] estimated SLD from surface parameters using an artificial neural network technique. Reference [26] investigated the seasonal variability of SLD in the central Arabian Sea. Using two climatologies, [27] studied the variability in the sound speed and the SOFAR channel in the Indian Ocean. Reference [28] used World Ocean Atlas (WOA01) climatology and Argo in situ data to study the distribution of the SLD in the Arabian Sea. Reference [29] used hourly mooring profiles and studied

the relative impact of temperature and salinity on the sound speed in the central Arabian Sea. Using the World Ocean Atlas 2013 (WOA13) annual data, [30] studied the variability of the sound channel over the BoB and Arabian Sea. Reference [31] used Argo data and studied the relationship between SLD and MLD in the Arabian Sea. Reference [32] studied the characteristics of the sound channel in the south central BoB. Reference [33] showed the afternoon effect in sound speed profiles in the central BoB using the high resolution Glider data.

Note, the variability of sound speed can also be analyzed from the climatology data. However, as the climatology fields are smooth and obtained from the long term average of data, the synoptic variabilities get diluted significantly. Because of the Argo project, the in-situ data coverage has significantly increased in the BoB. So, we have taken the opportunity to utilize the Argo observation data to capture the main properties (time and space scales, regionality, amplitudes, etc.) of the variability in the sound speed of the BoB upper ocean.

The main purpose of this study is to estimate the observed sound speed variability to (i) identify the regions and times of higher variabilities, and (ii) explore the sound speed structures and variabilities in different parts of the BoB.

The paper is organized as follows. Section II describes the data and the methodology used in this study. Section III presents the results on the sound speed variability. Section IV summarizes the study by highlighting the major findings.

II. DATA AND METHOD

A. Argo Data

The sound speed profiles in this study were estimated from the temperature and salinity profiles from the Argo observations over the period 2011 - 2020. The Argo data were obtained from the corioli's website (ftp://ftp.ifremer.fr/ifremer/argo/geo/indian_ocean). The Argo floats provide temperature and salinity data up to a depth of 2000m. All the Argo data are gone through several standard automated quality checks before being available for the users (in the webserver). All the Argo profiles were subjected to robust statistical and visual quality checks to remove the outliers and spurious values before using them for analysis in this study. We removed the profiles having data values outside two standard deviations from the mean profiles. The profiles, which have at least one observation within the upper 20m and extended down to 500 m and beyond, are considered in this study to make the spatial variability analysis consistent at different depths. A total of 14246 profiles were finally archived for this analysis over the 10-year period (Fig. 1). Month by month spatial distribution of the profiles are shown in Fig. 2. There is very little data available in the Andama Sea. However, other parts of the BoB have adequate data coverage in all the months.

B. Computation of Sound Speed

Due to unavailability of the direct measurements, the sound speed profiles were estimated from the Argo temperature and salinity profiles using the UNESCO equation [34]. All the temperature, salinity and sound speed profiles have been interpolated to a regular vertical grid with 1m resolution between 5m to 500m depths. The top depth is considered as 5 m because of there is a smaller number of data above this depth.

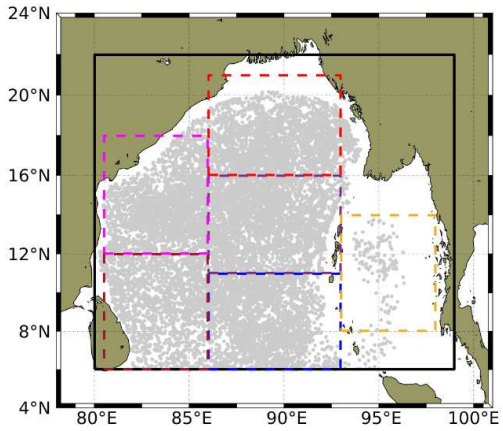

Fig. 1. Spatial distribution of all the Argo observations (grey dots) during 2011-2020 used in this study. The outer black box represents the study domain and the inner smaller boxes represent the sub-domains considered for the region-specific variability in sound speed. The definition of the domain and sub-domains are mentioned in Table 1.

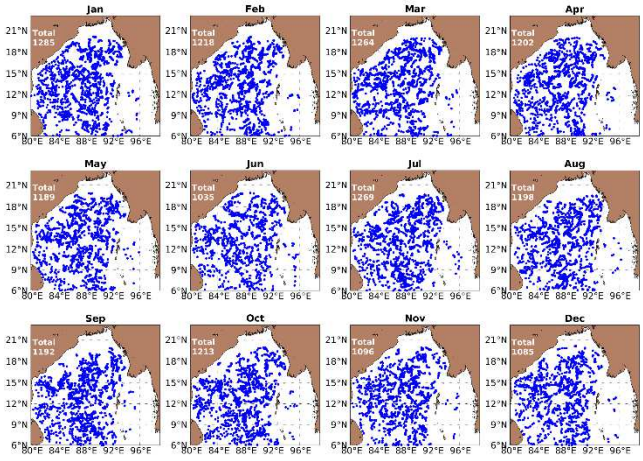

Fig. 2. Monthly maps of spatial distribution of Argo data used in the analysis. There are very little amount of data available in the Andaman Sea.

TABLE I. SPECIFICATION OF THE DOMAIN AND SUB-DOMAINS

Sub-Domain Names	Domain Boundaries	Description
BoB	$80-99°E; 6-23°N$	Entire domain Bay of Bengal
N-BoB	$86-93°E; 16-21°N$	Northern BoB
C-BoB	$86-93°E; 11-16°N$	Central BoB
S-BoB	$86-93°E; 6-11°N$	Southern BoB
CW-BoB	$80.5-86°E; 12-18°N$	Central Western BoB
SW-BoB	$80.5-86°E; 6-12°N$	South Western BoB
AS	$93-98°E; 8-14°N$	Andaman Sea

C. Selection of Domain and Subdomains

In order to study the region specific variability, we have divided the entire domain into subdomains. We considered six boxes (Fig. 1) covering most of the area of the domain, say North (N-BoB), South (S-BoB), Central (C-BoB), Central-West (CW-BoB), South-West (SW-BoB) and Andamas Sea (AS). These boxes are influenced by different oceanographic processes.

III. Results and Discussion

A. Domain-wide Variability

Fig. 3 presents the depth-dependent domain-wide spatio-temporal variability of the temperature, salinity and sound speed over the BoB. It is evident from the figure that the BoB temperature, salinity and sound speed present a wide range of variability over space and time. The temperature variability is largest in the thermocline layers while the salinity variability is largest in the surface layers. The sound speed also shows higher variability in the thermocline region with a maximum standard deviation (SD) of 6 m/s near 110 m depth. The pattern of sound speed variability follows that of the temperature, which indicates the dominant impact of temperature on sound speed on a domain-wide scale. The SD decreases towards the surface to a minimum of ~2.4 m/s near 35 m depth and again increases to ~3 m/s near the surface. Note, the variability at the surface is underestimated in this analysis as the observation is not available near the northern end where salinity variability is largest and has greater impact on sound speed. The range (maximum – minimum) of sound speed is around 20 m/s, while that goes to ~40 m/s in the thermocline depths.

To identify the regions of higher temporal variability at different depths, we present maps of mean (Fig. 4) and SD (Fig. 5) over a 1° × 1° regular horizontal grid at 5m, 35m, 110m and 500m depths. These depths are selected based on the higher and lower variabilities shown in Fig. 3. At each grid point, all the data within a 2° × 2° cell having the grid point at the centre are used in the mean and SD computation. Moreover, we have considered the only grids which contain data from all the twelve months and totalling at least 30 values to ensure statistical consistency.

Near the surface, the northern part of the BoB shows higher variability with a maximum of ~5 m/s, while the southern end shows the lowest variability. The distribution of this variability is quite consistent with the temperature and salinity variability. At 35m depth, the larger variability is seen in the northern end and southwestern part of the BoB. At this depth the salinity impact is smaller than that of the surface. At 110 m depth, the sound speed variability is significantly high and the spatial pattern of the variability is remarkably different from that on the surface. At this depth the largest variability is observed along the western boundary. The magnitude and the spatial pattern of this variability is consistent with those of the temperature variability confirming the dominant impact of temperature. Salinity variability and its impact on sound speed is negligible at this depth. At 500 m depth, the sound speed variability is very small (mostly less than 1.2 m/s) and follows the temperature variability.

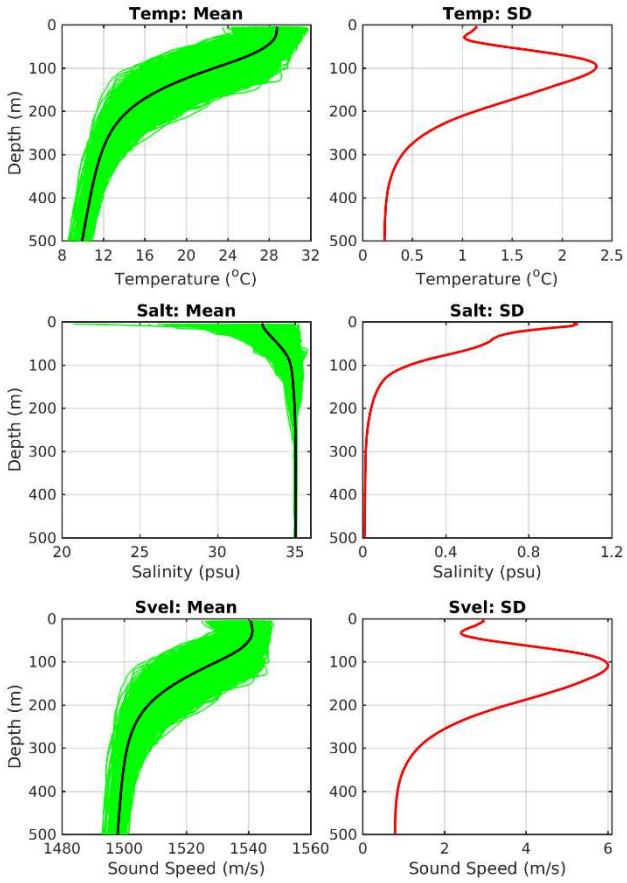

Fig. 3. Domain-wide spatio-temporal mean (left column: black line) and standard deviation (right column: red line) profiles of temperature (top row), salinity (middle row) and sound speed (bottom row) over the BoB obtained from all the Argo observations during 2011-2020. Green lines in the left column represent all the individual profiles of corresponding parameter

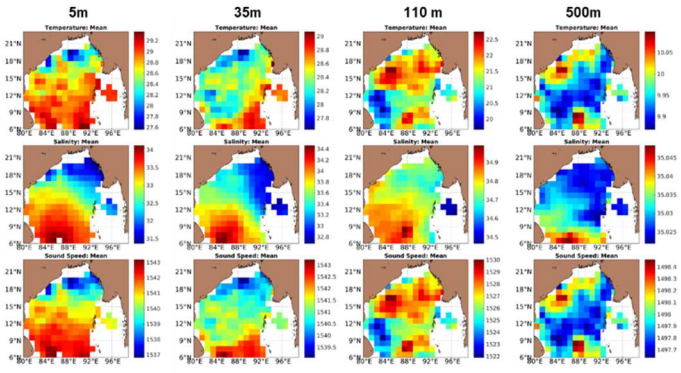

Fig. 4. Spatial maps of temporal mean of temperature (top row), salinity (middle row), and sound speed (bottom row) at 5m (left column), 35m (2nd column), 110m (3rd column) and 500m (last column).

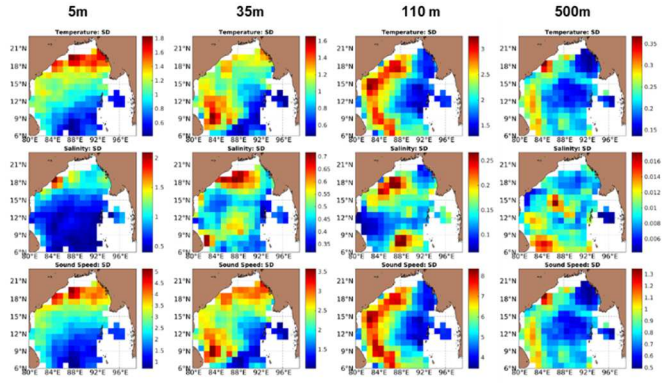

Fig. 5. Spatial maps of temporal standard deviation of temperature (top row), salinity (middle row), and sound speed (bottom row) at 5m (left column), 35m (2nd column), 110m (3rd column) and 500m (last column)

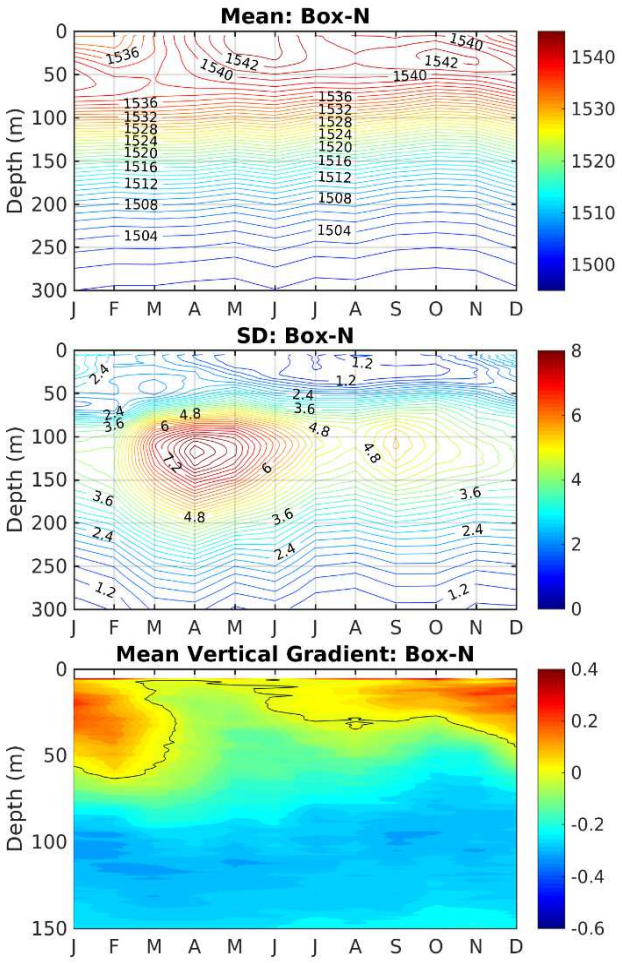

Fig. 6. Time depth variation of the spatio-temporal mean (top), standard deviation (middle) and vertical gradient of sound speed over the northern BoB (N-BoB) region.

B. Region Specific Variability

It is evident from the previous section that the sound speed variabilities vary significantly with regions. Moreover, different oceanographic processes affect the sound speed variability at different parts of the domain at different time scales. So, we divided the domain into multiple smaller subdomains (Fig. 1 and Table 1) to explain the region specific variabilities. We have considered six boxes covering almost the entire BoB as representatives of six sub-regions. At each of the boxes we have analyzed the month-depth variation of the mean and standard deviation of sound speed (Fig. 6-11). At each of the boxes, to compute the mean and standard deviation for a month, we considered the profiles of that month over all the years within the specific box. We also present the mean vertical gradient of the sound speed at each of the boxes.

Northern BoB: The northern BoB experiences a large variation in both temperature and salinity in the surface. Due to freshwater input from Ganges-Brahmaputra-Meghna (GBM) river system along with the monsoon rain reduces the salinity of this region throughout the year with a maximum intensity during monsoon and postmensoon period. Due to this freshwater induced stratification in the surface layers results in barrier layer formation below the mixed layer. Heat gets trapped within the barrier layer that eventually leads to the formation of subsurface temperature inversion in the winter. In addition, the surface temperature in this region drops significantly during the winter and experiences the lowest temperature in the domain.

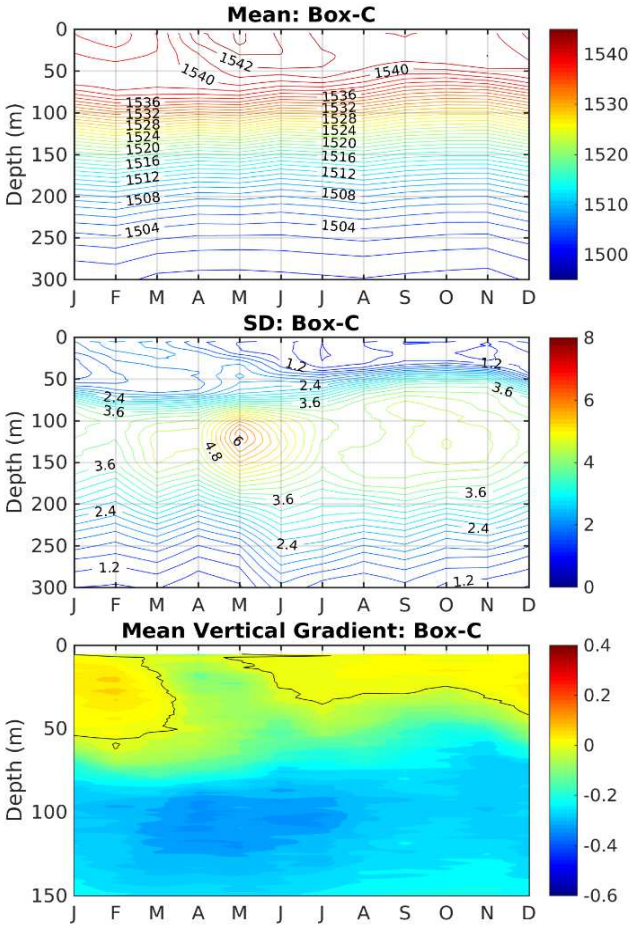

Fig. 7. Same as Fig. 6 but for central BoB (C-BoB) region.

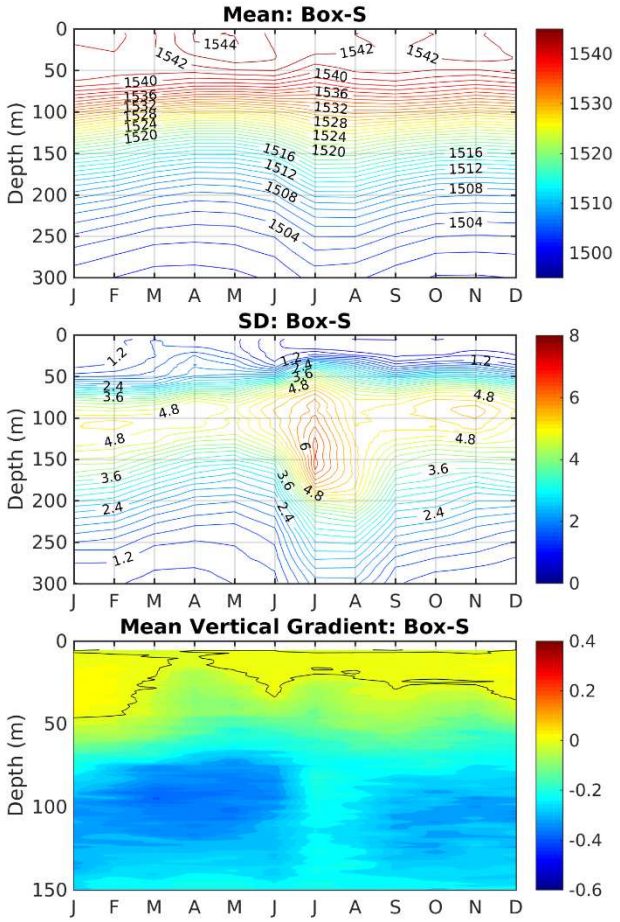

Fig. 8. Same as Fig. 6 but for south BoB (S-BoB) region.

Fig. 6 shows the sound speed variability in the northern BoB. The average sound speed on the surface is maximum (~1544 m/s) during May when the surface temperature is maximum and the freshwater impact is minimum. After the onset of summer monsoon in June, the supply of freshwater from rivers and rain increases, which reduces the salinity and eventually the sound speed. Note, the signature of the freshwater impact in terms of lower salinity in June is not evident due to lack of the data close to GBM river mouth. During the winter, the surface temperature drops and hence the sound speed. The impact of cold temperature along with the lower salinity leads to the lowest surface sound speed during the winter (~1533 in January-February).

The sound speed in this region shows a prominent subsurface maxima (Fig. 6 top) associated with positive vertical gradient (Fig. 6 bottom) throughout the year except during April-May. Due to hydrostatic pressure, the sound speed increases with depth within the mixed layer. However, in this region, the temperature and salinity is more responsible for this subsurface maxima than the hydrostatic pressure. Higher salinity gradient in the stratified layer results in enhanced vertical gradient in the sound speed. In addition, during the winter the presence of temperature inversion substantially enhances the subsurface maxima. The subsurface maxima and the corresponding positive gradient in sound speed is largest during the winter which is the combined impact of temperature inversion and the salinity stratification. This large positive gradient results in upward refraction of sound and has a significant implication on formation of surface ducting and shadow zone. Note, the sound speed in the deeper layers of this region does not show any significant seasonal variation. The variability in the sound speed is seen to be higher in the thermocline layers. This variability is substantially large during the spring with a maximum intensity (~8.3 m/s) near 115-120 m depth during April. Another moderate peak in this layer can be seen in September. At the surface, the variability is higher during the winter.

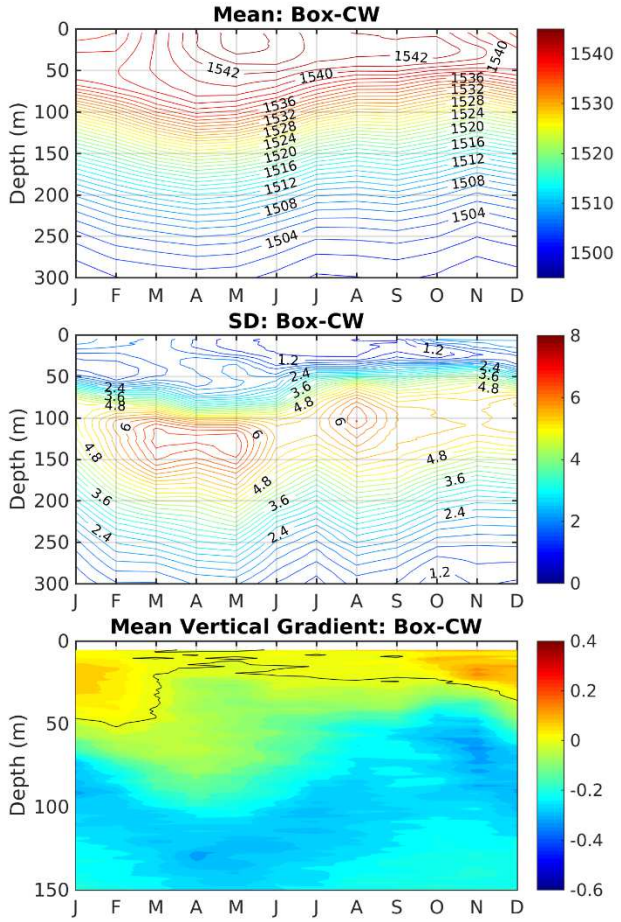

Fig. 9. Same as Fig. 6 but for central west BoB (CW-BoB) region.

Central BoB: This region is free from any direct impact from major oceanic processes of the BoB, such as freshwater plume, equatorial currents, boundary currents and the coastal upwelling. The region does not show any specific circulation features, rather mostly affected by several eddies. As the central BoB is the link between the fresher northern part and saltier southern part, it shows moderate salinity variation. Fig. 7 demonstrates the sound speed variability in the central BoB region. The average surface sound speed ranges from 1537 m/s in February to 1544 m/s in May. The positive vertical gradient is very weak in this region. There is no signature of positive gradient during March-May indicating the absence of a sonic

layer during this time. The moderately higher vertical gradient in February is due to the presence of the temperature inversion in the northern part of this region along with comparatively lower surface salinity. The variability in the thermocline depth is weak compared to the other regions of the BoB. The maximum variability (~6.2 m/s) is seen in May near 125 m depth.

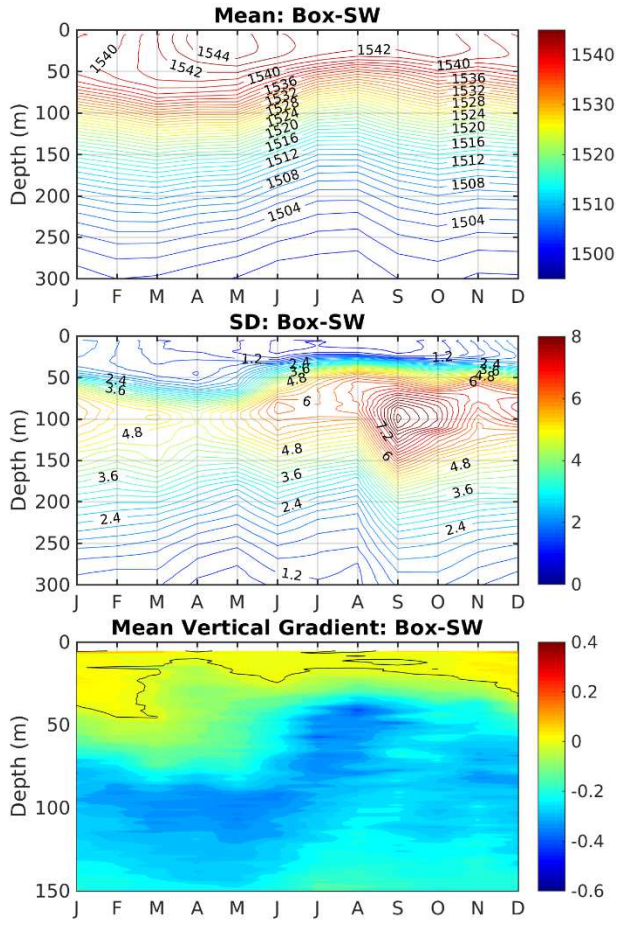

Fig. 10. Same as Fig. 6 but for southwest BoB (SW-BoB) region.

Southern BoB: The southern Bay is influenced by the equatorial Indian Ocean processes. The surface layers remain warmer and saltier compared to the northern BoB throughout the year. The sound speed variability in this region is shown in Fig. 8. The vertical salinity gradient remains small. The average surface sound speed remains higher throughout the year and shows very little seasonal variation with maximum (~1544 m/s) in April-May and minimum (~1541 m/s) in January-February. The subsurface maxima is mostly diluted and the positive vertical gradient is very small. During March-April, there is no clear signature of positive gradient and hence the sonic layer depth. The largest variability could be seen in the thermocline depth with a maximum (~6.4 m/s) in July near 120-170 m depth.

Western BoB: The western part of the BoB is influenced by the seasonally reversing western boundary currents and a number eddies throughout the year. The Figures 9 and 10 show the sound speed variations over the central and southern part of the western BoB respectively. The average surface sound speed in the central (southern) part ranges from ~1537 m/s (~1539 m/s) in January-February to ~1545 m/s in May (April-May). The surface sound speed in the central part is lower than that in the southern part. The subsurface maxima is more prominent with stronger positive vertical gradients in the central part than that in the southern part. This is due to the greater freshwater impact in the central part. The EICC carries low saline water in the southern part during October-December. Note, below the SLD, the intensity of the negative vertical gradient shows a clear seasonality in the western BoB. The negative gradient is greater in the southern part than the central part. The occurrence of the higher variability in the thermocline region is different in the central and southern part. The maximum variability in the central part occurs during March-May near 125 m depth, while that in the southern part occurs during September-October near 100m depth.

Andaman Sea: In the Andaman Sea region we have very little data, which does not provide enough confidence to conclude about the sound speed variability of the region. However, we present the variability analysis in Figure 11 from the available data to provide an indication.

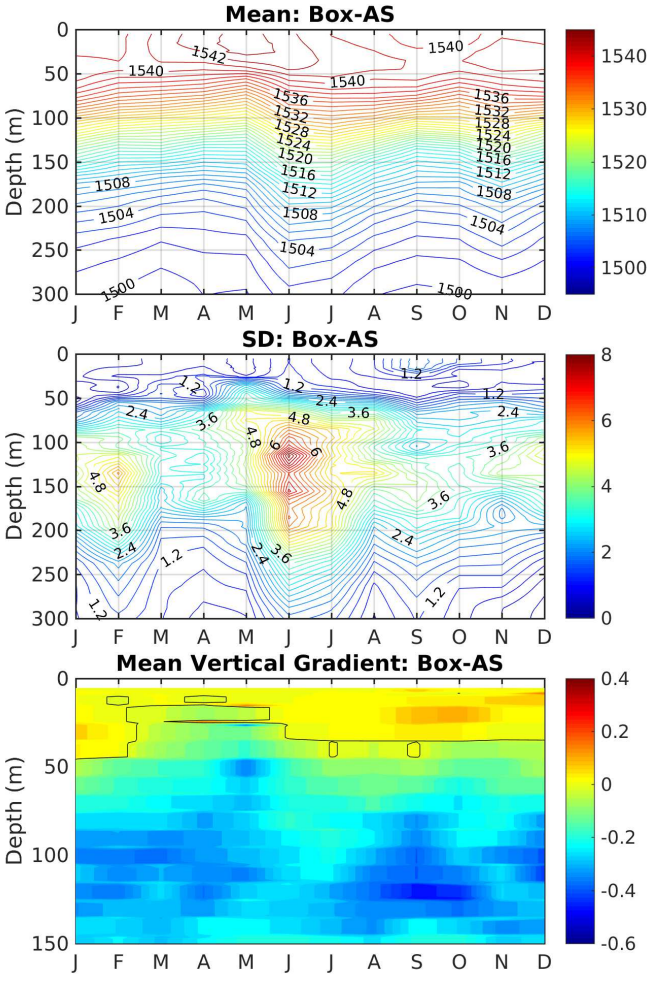

Fig. 11. Same as Fig. 6 but for Andaman Sea (AS) region.

IV. Summary and Conclusion

Understanding of sound speed structure and its variability is very important for underwater acoustic propagation and its applications in any oceanic region. Several oceanographic processes result in substantial variation in the temperature and salinity over space and time which eventually modulates the sound speed of the BoB. The sound speed variability estimated from classic climatological data cannot be easily utilized to capture the synoptic variability. In this study, we present the sound speed variability of the BoB from direct historical Argo observations over a 10-year period spanning from 2011 to 2020. Our study mostly focused on the variability within the upper 500m. Specifically, we have analyzed the variability in the domain-wide and region specific sound speed structures and identified the regions where the sound speed variability is significant. It is evident that the domain wide sound speed variation is maximum in the thermocline layers due to the temperature variation. In the surface layers, the higher sound speed variation is seen in the northern part while that in the thermocline region is seen along the western boundary of the Bay. The temperature is found to be the dominant factor to determine the overall sound speed structure and variability; however, the salinity has a significant impact in the near-surface layers. In order to characterize the regional variations, we divided the BoB in six subdomains and investigated the sound speed structure and variability in each of these subdomains. The sound speed variations at different parts of the Bay varies with time and depth. The larger variabilities are observed in the northern and western part of the BoB. In the northern and central-sestern BoB show larger variabilities during the spring time within mostly within ~100-150 m depth. In the southwestern BoB, the larger variability is observed during the postmonsoon period within ~70-130 m depth. Northern BoB shows lower sound speed in the surface and a prominent subsurface maxima during major part of the year except pre-monsoon period. The distribution of the variability in the northern BoB shows the largest positive vertical gradient above the sonic layer depth (SLD) which is favourable for formation of the shadow zone below the SLD.

The present results highlight the importance of understanding the sound speed variation in the BoB from observations. The study can be extended further to understand the variability in the SLD and the deep sound channel. In addition, our findings will help perform acoustic modeling [35] – [38] in the BoB and its regions. It is also useful to extend data in space for mapping [39], [40] and to develop feature models [41]. Characterizing the variability by ocean region is also essential for accurate uncertainty initialization, probabilistic forecasting and data assimilation, with varied ocean acoustic applications [42] – [45]. In the future, our results can be used for stochastic dynamically-orthogonal acoustic predictions [46], [47] and adaptive sampling [48]. Additional ocean acoustics studies would be most useful for the region, ideally integrating ocean modeling and sustained in-situ sensing with autonomous platforms [49], as for the Northern Arabian Sea [50], [51] adjacent to the BoB. Such studies would lead to further understanding of the BoB dynamics and its influence on weather and climate, and the results could benefit local populations, marine industries, and security in the region.

Acknowledgment

We thank the Argo teams for collecting data, performing quality control and making the data available for use. PFJL and PJH are grateful to the Office of Naval Research for partial support under Grants N00014-19-1-2693 (IN-BDA) and N00014-19-1-2664 (TFO: DEEP-AI) to the Massachusetts Institute of Technology (MIT).

References

[1] V. S. N. Murty, Y. V. B. Sarma, D. P. Rao, and C. S. Murty, "Water characteristics, mixing and circulation in the Bay of Bengal during southwest monsoon," *Journal of Marine Research*, vol. 50, no. 2, pp. 207–228, 1992.

[2] S. R. Shetye, "The movement and implications of the Ganges-Bramhaputra runoff on entering the Bay of Bengal," *Curr. Sci.*, vol. 64, no. 1, pp. 32–38, 1993.

[3] P. N. Vinayachandran and J. Kurian, "Hydrographic observations and model simulation of the Bay of Bengal freshwater plume", *Deep Sea Res. I*, vol. 54, pp. 471–486, 2007

[4] S. Jana, A. Gangopadhyay and A. Chakraborty, "Impact of Seasonal River Input on the Bay of Bengal Simulation," *Continental Shelf Research*, vol. 104, pp. 45-62, 2015.

[5] A. Behara, and P. N. Vinayachandran. "An OGCM study of the impact of rain and river water forcing on the Bay of Bengal," *Journal of Geophysical Research: Oceans,* vol. 121, no. 4, pp. 2425-2446, 2016.

[6] S. Jana, A. Gangopadhyay, P.F. Lermusiaux, A. Chakraborty, S. Sil and P.J. Haley Jr., "Sensitivity of the Bay of Bengal upper ocean to different winds and river input conditions," *Journal of Marine Systems*, vol. 187, pp. 206-222, 2018.

[7] P. N. Vinayachandran, V. R. Babu, and V. S. N. Murty, "Observations of barrier layer formation in the Bay of Bengal during summer monsoon," *J. Geophys. Res.*, vol. 107(C12), 2002. doi:10.1029/2001JC000831.

[8] P. Thadathil, V. V. Gopalakrishna, P. M. Muraleedharan, G. V. Reddy, N. Araligidad, and S. Shenoy, "Surface layer temperature inversion in the Bay of Bengal," *Deep Sea Res. I*, vol. 49, pp. 1801–1818, 2002.

[9] B. Thompson, C. Gnanaseelan, and P. S. Salvekar, "Seasonal evolution of temperature inversions in the north Indian Ocean," *Current Science*, vol. 90, no. 5, pp. 697–704, 2006.

[10] P. Thadathil, P. M. Muraleedharan, R. R. Rao, Y. K. Somayajulu, G. V. Reddy, and C. Revichandran, "Observed seasonal variability of barrier layer in the Bay of Bengal," *Journal of Geophysical Research*, vol. 112(C02009), 2007. doi:10.1029/2006JC003651.

[11] M. S. Girishkumar, M. Ravichandran, and M. J. McPhaden. "Temperature inversions and their influence on the mixed layer heat budget during the winters of 2006–2007 and 2007–2008 in the Bay of Bengal." *Journal of Geophysical Research: Oceans,* vol. 118, no. 5, pp. 2426-2437, 2013.

[12] P. Kurien, M. Ikeda, and V. K. Valsala, "Mesoscale variability along the east coast of India in spring and fall revealed in satellite data and OGCM," *Journal of Oceanography*, vol. 66, pp. 273–289, 2010.

[13] S. Sil, A. Chakraborty and M. Ravichandran, "Numerical Simulation of Surface Circulation Features Over the Bay of Bengal using Regional Ocean Modeling System," *Adv. GeoSci.*, vol. 24, pp.117 – 130, 2011.

[14] A. Gangopadhyay, G. N. Bharat Raj, A. H. Chaudhuri, M. T. Babu, and D. Sengupta, "On the nature of meandering of the springtime western boundary current in the Bay of Bengal," *Geophys. Res. Lett.*, vol. 40, pp. 2188–2193, 2013. doi:10.1002/grl.50412.

[15] S. R. Shetye, A. D. Gouveia, D. Shankar, S. S. C. Shenoi, P. N. Vinayachandran, D. Sundar, G. S. Michael, and G. Nampoothiri. "Hydrography and circulation in the western Bay of Bengal during the northeast monsoon, " *Journal of Geophysical Research: Oceans*, vol. 101, no. C6, pp. 14011-14025, 1996.

[16] S. R. Shetye, S. S. C. Shenoi, A. D. Gouveia, G. S. Michael, D. Sundar, and G. Nampoothiri, "Wind-driven coastal upwelling along the western boundary of the Bay of Bengal during the southwest monsoon," Continental Shelf Research, vol. 11, no. 11, pp. 1397-1408, 1991.

[17] P. N. Vinayachandran, D. Shankar, S. Vernekar, K. K. Sandeep, P. Amol, C. P. Neema, and A. Chatterjee, "A summer monsoon pump to keep the Bay of Bengal salty," Geophysical *Research Letters,* vol. 40, no. 9, pp. 1777-1782, 2013.

[18] B. G. Webber, A. J. Matthews, P. N. Vinayachandran, C. P. Neema, A. Sanchez-Franks, V. Vijith, P. Amol, and D. B. Baranowski, "The dynamics of the Southwest Monsoon Current in 2016 from high-resolution in situ observations and models," *Journal of Physical Oceanography,* vol. 48, no. 10, pp. 2259-2282, 2018.

[19] R. R. Rao, M. S. Girish Kumar, M. Ravichandran, A. R. Rao, V. V. Gopalakrishna, and P. Thadathil, "Interannual variability of Kelvin wave propagation in the wave guides of the equatorial Indian Ocean, the coastal Bay of Bengal and the southeastern Arabian Sea during 1993–2006," *Deep Sea Research Part I: Oceanographic Research Papers,* vol. 57, no. 1, pp. 1-13, 2010.

[20] A.R. Robinson, P.F.J. Lermusiaux and N.Q. Sloan, III, "Data Assimilation," *The Sea: The Global Coastal Ocean I, Processes and*

Methods (K.H. Brink and A.R. Robinson, Editors), Volume 10, John Wiley and Sons, New York, NY, pp. 541-594, 1998.

[21] A.R. Robinson and P.F.J. Lermusiaux, "Data Assimilation in Models. Encyclopedia of Ocean Sciences," *Academic Press Ltd., London*, 623-634, 2001.

[22] A.R. Robinson, and P.F.J. Lermusiaux, "Prediction Systems with Data Assimilation for Coupled Ocean Science and Ocean Acoustics," *Proceedings of the Sixth International Conference on Theoretical and Computational Acoustics (A. Tolstoy, et al., editors)*, World Scientific Publishing, pp. 325-342, 2004.

[23] S. K. Sinha, P. Dewangan, and K. Sain. "Acoustic reflections in the water column of Krishna-Godavari offshore basin, Bay of Bengal." *The Journal of the Acoustical Society of America* 139, no. 5 (2016): 2424-2431.

[24] S. Prasanna Kumar, G.S. Navelkar, T.V. Murty, Y.K. Somayajulu and C.S. Murty, "Sound speed structure in the Arabian Sea and the Bay of Bengal" , 1993

[25] S. Jain, M. M. Ali, and P. N. Sen, "Estimation of sonic layer depth from surface parameters," *Geophysical Research Letters*, vol. 34, pp. 17, pp. L17602, 2007.

[26] T. V. S. U. Bhaskar, D. Swain, and M. Ravichandran, "Seasonal variability of sonic layer depth in the central arabian sea," *Ocean Science Journal*, vol. 43, no. 3, pp. 147-152, 2008.

[27] V. S. Swaminathan, and P. K. Bhaskaran, "Variability in Sound Speed Structure and SOFAR Channel Depth in the Indian Ocean," *Journal of Ship Technology*, vol. 5, no. 1, pp. 53-72, 2009.

[28] T. U. Bhaskar, D. Swain and M. Ravichandran, "Sonic layer depth variability in the Arabian Sea," *International Journal of Oceans and Oceanography*, vol. 4, no. 1, pp. 17-28, 2010.

[29] M.M. Ali, S. Jain and R. Ramachandran, "Effect of temperature and salinity on sound speed in the central Arabian Sea," *The open Ocean Engineering Journal*, vol. 4, no. 1, pp. 71-76, 2011.

[30] Ashalatha, K., T. V. R. Murty, and K. V. S. R. Prasad. "Spatial Distribution of Sound Channel and Its Parameters in North Indian Ocean." Journal of Shipping and Ocean Engineering 5 (2015): 334-340.

[31] T. V. S. Bhaskar and D. Swain, "Relation between Sonic Layer and Mixed layer depth in the Arabian Sea," *Indian Journal of Geo-Marine Science*, vol. 45, no. 10, pp. 1264-1271, 2016.

[32] P. V. Hareesh Kumar, "The sound channel characteristics in the south central Bay of Bengal," *International Journal of Innovative Technology and Exploring Engineering*, vol. 3, pp. 61-5, 2013.

[33] S. Zacharia, R. Seshasayanan, T. Sudhakar, M. A. Atmanand, and R. R. Rao, "Observed variability of surface layer in the Central Bay of Bengal: results of measurements using glider," *Current Science*, pp. 2151-2159, 2017.

[34] N. P. Fofonoff, and R. C. Millard Jr, "Algorithms for the computation of fundamental properties of seawater", (Unesco, Paris, France, 1983), 53 pp., 1983.

[35] F.P Lam, P.J. Haley, Jr., J. Janmaat, P.F.J. Lermusiaux, W.G. Leslie, and M.W. Schouten, "At-sea Real-time Coupled Four-dimensional Oceanographic and Acoustic Forecasts during Battlespace Preparation 2007" *Special issue of the Journal of Marine Systems on "Coastal processes: challenges for monitoring and prediction",* Drs. J.W. Book, Prof. M. Orlic and Michel Rixen (Guest Eds.), vol. 78, pp. S306-S320, 2009. doi: 10.1016/j.jmarsys.2009.01.029.

[36] P. F. J. Lermusiaux, J. Xu, C. F. Chen, S. Jan, L. Y. Chiu, and Y. J. Yang, "Coupled ocean–acoustic prediction of transmission loss in a continental shelfbreak region: Predictive skill, uncertainty quantification, and dynamical sensitivities," *IEEE Journal of Oceanic Engineering,* vol. 35, no. 4, pp. 895-916, 2010.

[37] T.F. Duda, Y.-T. Lin, A.E. Newhall, K.R. Helfrich, W.G. Zhang, M. Badiey, P.F.J. Lermusiaux, J.A. Colosi, and J.F. Lynch, "The Integrated Ocean Dynamics and Acoustics (IODA) Hybrid Modeling Effort," *Proceedings of the international conference on Underwater Acoustics* - 2014 (UA2014), pp. 621-628, 2014.

[38] T. F. Duda, Y.-T. Lin, A. E. Newhall, K. R. Helfrich, J. F. Lynch, W. G. Zhang, P. F J Lermusiaux, and J. Wilkin, "Multiscale multiphysics data-informed modeling for three-dimensional ocean acoustic simulation and prediction," *The Journal of the Acoustical Society of America,* vol. 146, no. 3, pp. 1996-2015, 2019.

[39] P.F.J. Lermusiaux, D.G.M. Anderson and C.J. Lozano, "On the mapping of multivariate geophysical fields: error and variability subspace estimates," *The Quarterly Journal of the Royal Meteorological Society*, April B, pp. 1387-1430, 2000.

[40] Y.-T. Lin, A.E. Newhall, T.F. Duda, P.F. J. Lermusiaux and P.J. Haley, Jr., "Merging Multiple Partial-Depth Data Time Series Using Objective Empirical Orthogonal Function Fitting," *IEEE Transactions, Journal of Oceanic Engineering,* vol. 35, no. 4, pp. 710-721, 2010. doi:10.1109/JOE.2010.2052875.

[41] A. Gangopadhyay, P.F.J. Lermusiaux, L. Rosenfeld, A.R. Robinson, L. Calado, H.S. Kim, W.G. Leslie and P.J. Haley, Jr., "The California Current System: A Multiscale Overview and the Development of a Feature-Oriented Regional Modeling System (FORMS)," *Dynamics of Atmospheres and Oceans*, vol. 52, pp. 131-169, 2011. doi:10.1016/j.dynatmoce.2011.04.003.

[42] P.F.J., Lermusiaux, "Uncertainty Estimation and Prediction for Interdisciplinary Ocean Dynamics," Refereed manuscript, Special issue on "Uncertainty Quantification". J. Glimm and G. Karniadakis, Eds. Journal of Computational Physics, vol. 217, pp. 176-199, 2006. doi: 10.1016/j.jcp.2006.02.010

[43] C. Evangelinos, P.F.J. Lermusiaux, J. Xu, P.J. Haley, and C.N. Hill, "Many Task Computing for Real-Time Uncertainty Prediction and Data Assimilation in the Ocean," *IEEE Transactions on Parallel and Distributed Systems,* Special Issue on Many-Task Computing, I. Foster, I. Raicu and Y. Zhao (Guest Eds.), vol. 22, 2011. doi: 10.1109/TPDS.2011.64

[44] P.F.J. Lermusiaux, P.J. Haley, Jr., C. Mirabito, W.H. Ali, M. Bhabra, P. Abbot, C.-S. Chiu, and C. Emerson, "Multi-resolution Probabilistic Ocean Physics-Acoustic Modeling: Validation in the New Jersey Continental Shelf" In: OCEANS '20 IEEE/MTS, 5-30 October 2020, pp. 1-9. doi:10.1109/IEEECONF38699.2020.9389193

[45] P.F.J. Lermusiaux, C. Mirabito, P.J. Haley, Jr., W.H. Ali, A. Gupta, S. Jana, E. Dorfman, A. Laferriere, A. Kofford, G. Shepard, M. Goldsmith, K. Heaney, E. Coelho, J. Boyle, J. Murray, L. Freitag, and A. Morozov, "Real-time Probabilistic Coupled Ocean Physics-Acoustics Forecasting and Data Assimilation for Underwater GPS", OCEANS '20 IEEE/MTS, 5-30 October 2020, pp. 1-9. doi:10.1109/IEEECONF38699.2020.9389003

[46] W.H. Ali, M.S. Bhabra, P.F.J. Lermusiaux, A. March, J.R. Edwards, K. Rimpau, and P. Ryu, "Stochastic Oceanographic-Acoustic Prediction and Bayesian Inversion for Wide Area Ocean Floor Mapping," OCEANS '19 MTS/IEEE Seattle, 27-31 October 2019, doi:10.23919/OCEANS40490.2019.8962870

[47] A. Charous and P.F.J. Lermusiaux, "Dynamically Orthogonal Differential Equations for Stochastic and Deterministic Reduced-Order Modeling of Ocean Acoustic Wave Propagation," OCEANS '21 IEEE/MTS San Diego, 20-23 September 2021, pp. 1-7, in press, 2021.

[48] D. Wang, P.F.J. Lermusiaux, P.J. Haley, D. Eickstedt, W.G. Leslie and H. Schmidt, "Acoustically Focused Adaptive Sampling and On-board Routing for Marine Rapid Environmental Assessment," Special issue of Journal of Marine Systems on "Coastal processes: challenges for monitoring and prediction", Drs. J.W. Book, Prof. M. Orlic and Michel Rixen (Guest Eds), vol. 78, pp. S393-S407, 2009. doi: 10.1016/j.jmarsys.2009.01.037

[49] O. Schofield, S. Glenn, J. Orcutt, M. Arrott, M. Meisinger, A. Gangopadhyay, W. Brown, R. Signell, M. Moline, Y. Chao, S. Chien, D. Thompson, A. Balasuriya, P.F.J. Lermusiaux and M. Oliver, "Automated Sensor Networks to Advance Ocean Science," EOS, vol. 91, no. 39, 28 September 2010.

[50] L.R. Centurioni, V. Hormann, L. D. Talley, I. Arzeno, L. Beal, M. Caruso, P. Conry, R. Echols, H. J. S. Fernando, S. N. Giddings, A. Gordon, H. Graber, R. Harcourt, S. R. Jayne, T. G. Jensen, C. M. Lee, P. F. J. Lermusiaux, P. L'Hegaret, A. J. Lucas, A. Mahadevan, J. L. McClean, G. Pawlak, L. Rainville, S. Riser, H. Seo, A. Y. Shcherbina, E. Skyllingstad, J. Sprintall, B. Subrahmanyam, E. Terrill, R. E. Todd, C. Trott, H. N. Ulloa, and H. Wang, "Northern Arabian Sea Circulation-Autonomous Research (NASCar): A Research Initiative Based on Autonomous Sensors. Oceanography," vol. 30, no. 2, pp. 74–87, 2017. https://doi.org/10.5670/oceanog.2017.224

[51] P.F.J. Lermusiaux, P.J. Haley Jr., S. Jana, A. Gupta, C.S. Kulkarni, C. Mirabito, W.H. Ali, D.N. Subramani, A. Dutt, J. Lin, A. Y. Shcherbina, C. M. Lee, and A. Gangopadhyay, "Optimal Planning and Sampling Predictions for Autonomous and Lagrangian Platforms and Sensors in the Northern Arabian Sea," Oceanography, vol. 30, no. 2, pp. 172–185, 2017. https://doi.org/10.5670/oceanog.2017.242.